UNIVERSITY OF TWENTE.

Technical Medicine

Master thesis

In silico modeling of patients with type 1 diabetes mellitus

A.J. Onvlee

Graduation Committee

Prof. dr. H.J. Zwart
Dr. A.C. van Bon
Dr. M. Groenier
Dr. ir. W.L. van Meurs
H. Blauw, MSc

September 21, 2016

A.J. Onvlee

In silico modeling of patients with type 1 diabetes mellitus

Master thesis, September 21, 2016
Technical supervisors: Prof. dr. H.J. Zwart and H. Blauw, MSc
Medical supervisor: Dr. A.C. van Bon
Process supervisors: Dr. M. Groenier

University of Twente
Technical Medicine
Drienerlolaan 5
7522 NB Enschede, The Netherlands

Abstract

For the development and testing processes of a medical device, a simulation model can be helpful. Inreda Diabetic BV (Goor, The Netherlands) is developing an artificial pancreas to regulate the blood glucose value in patient with type 1 diabetes mellitus. This new medical device is a bi-hormonal closed-loop system. A simulation model was designed to test the algorithm of the artificial pancreas. The aim of this study was to develop a model to help understand the medical device interactions on the glucose regulation and to provide information on the simulated responses to various stimuli. The model represents the three main physiological subsystems, the glucose, insulin and glucagon processes. In addition, the first simulation results proved that the model can simulate the glucose regulation, albeit with parameters from literature. Next, a first step was made to estimate the model's parameters. However, these estimations are not straightforward and further research is necessary. Despite this limitation, this study showed a solid developed model for the understanding of the glucose regulation.

Contents

1 Introduction

1.1 Diabetes management

Diabetes mellitus is a chronic metabolic disorder resulting in a dysfunctional glucose regulation. In type 1 diabetes, the β-cells in the pancreas are affected by an autoimmune response [9, 37]. This leads to necrosis of the β-cells, which results in reduced cell mass. As a consequence, the β-cells fail to secrete (enough) insulin. At this moment there is no cure for diabetes. Pellegrini et al. identified that the affected β-cells can be replaced by healthy β-cells [28]. These islet transplantations can be done by different methods [28]. The transplantation methods still have its limitations that need to be overcome, before there will be a cure for diabetes.

Therefore, the management of diabetes is focused on maintaining the patient's blood glucose within the desired range. Patients need to regulate their own blood glucose by measuring and correcting their blood glucose levels. A high blood glucose level, or hyperglycemia, is corrected by injecting insulin. Hypoglycemia, which is a low blood glucose level, can be corrected by eating carbohydrates. Further, they need to keep in mind what to eat or when to exercise. This self-regulation requires considerable effort from the patient. Patients are constantly managing their blood glucose levels [19]. This requires an adaptation of their lifestyles [19]. Diabetes has a great impact on the patient's lifestyle [21] and their families [34].

As mentioned above, patients need to measure their blood glucose values to manage their diabetes. A device for Self Monitoring of Blood Glucose (SMBG) helps with this measurement. The device works with a drop of blood derived from a finger prick and reports the glucose value. On the basis of this measurement the patient can correct a high glucose value by the administration of insulin. A low value is mostly corrected by eating carbohydrates. These actions are preformed several times a day: mostly before meals and before bedtime. Insulin is given subcutaneously by pen, called Multiple Daily Insulin (MDI) therapy, or by insulin pump called Continuous Subcutaneous Insulin Infusion (CSII). MDI is the common therapy for type 1 diabetes mellitus (T1DM) patients.

Medical devices for diabetes disease management can relieve the patient's burden. One of these devices is a glucose sensor: Continuous Glucose Monitors (CGM).

This is an amperometric biosensor for the continuous measurement of the glucose concentration in the interstitial fluid. The glucose level in the interstitial fluid corresponds to the subcutaneous glucose values. These measurements provide patients more insight in their own blood glucose values than irregular SMBG blood glucose measurements. The CGM displays not only the values, but also the trends and rate of change. Nevertheless, the interpretation and treatment decisions need to be done by the patient [19]. With the use of CGM, less SMBG measurements have to be performed. The SMBG measurements are only needed for calibration or to verify the glucose sensor.

The insulin pump, CSII, is also a medical device in diabetes management. This device provides continuous subcutaneous insulin administration and bolus insulin before the intake of carbohydrates. Once per 2 days the infusion set of the CSII needs to be replaced. Therefore, the burden of frequent insulin administration is diminished compared to MDI. Another advantage of CSII is the ability to adjust the basal insulin infusion rate. In contrast to MDI where the long acting insulin is given once a day and cannot be adjusted during the day or night. Therefore, patients with frequent hypoglycemia and/or hypoglycemia unawareness benefit from CSII therapy [22]. CSII therapy delivers only insulin, patients still need to count carbohydrates and decide on the amount of bolus insulin. This extra-administered insulin minimizes or corrects peaks in the blood glucose value. The bolus is complementary to the basal insulin.

CSII can be combined with SMBG systems. The blood glucose values are automatically sent from the SMBG to the CSII device. CSII features can support the patient with calculating the bolus of insulin using the amount of carbohydrates, the current glucose value and the insulin levels. Even with this support, named bolus calculator, patients still need to take care of their own therapy: measuring glucose with a finger prick, counting carbohydrates and entering these results in the bolus calculator, taking into account any intended physical activity.

1.2 Closed loop systems

In sensor-augmented pump therapy the CGM and CSII systems are combined. This is a prospect of a closed-loop system. A closed-loop system automatically controls the desired output. The controller responds to changing output, without any human intervention. The closed-loop system includes a sensor to measure these changes. In case of a closed-loop system for diabetes management the controlled output is the blood glucose value, which should remain in a specified range. The controller is a medical device, for instance the CSII with a glucose control algorithm, and the CGM

is the sensor. The continuous development of the technology behind the CGM and CSII contributes to the closed-loop principle [19, 32]. The two connected devices replace the pancreatic function of sensing and controlling the glucose regulation.

Inreda Diabetic BV (Goor, The Netherlands) is developing a closed-loop system, i.e. an artificial pancreas (AP) [2]. The goal is to regulate the blood glucose value [17] in order to prevent hyperglycemia and hypoglycemia. The system is bi-hormonal, because it can administer insulin and glucagon. Insulin and glucagon are counter-regulatory hormones, their action is to prevent hyper- and hypoglycemia, respectively. Therefore this device contains two pumps for the insulin and glucagon delivery. The use of glucagon is an expansion of CSII. The rationale for using glucagon in the closed loop is that the glucagon response to hypoglycemia is compromised in diabetes [20]. Therefore, glucagon secretion by the α-cells is supported or replaced by the closed-loop controller. Furthermore the AP uses two CGMs to improve the measurement's accuracy and reliability. The algorithm of the controller calculates the required doses of either insulin or glucagon to adjust the glucose values.

1.3 Models

Not only technological advancements are important, mathematical models can also have a significant impact on the development of a closed-loop system. A model is a representation of the reality involving some degree of approximation. Therefore, a model is a simplification of the reality. A model can achieve four types of goals [7, 10]: describing quantitative relationships in terms of equations, interpreting experimental results, predicting a system response to a certain stimulus, or explain the change to an observation or measurement. The model goal determines the modeling method.

A mathematical model describes the physiological behavior in terms of mathematical equations. This model type can be based on clinical data or on the understanding of the physiological process. The first modeling method is called a black box. The mathematical description of the physiology is identified with experimental input and output data. For the second method, it is necessary to understand the physiological complexity in order to make conscious decisions. Decisions are based on simplifications and assumptions. This modeling method is called a white box. However, the physiology is seldom entirely understood and not all the parameters can be directly measured [7]. For these two reasons the physiology is often modeled as a grey box.

A model can be helpful in the development and testing processes for medical devices.

The model helps to understand the medical device interactions on a physiological process. It provides information on the simulated responses to various stimuli of the medical device. A model also simulates a wider range of physiological and pathophysiological situations than can be tested in clinical trials. Therefore, it is a valuable tool for preclinical testing of a medical device.

Clinical studies are important to determine the safety and performance of the glucose control algorithm of the closed-loop system. Only, the development, evaluation and testing of the control algorithm is time consuming, expensive and it involves ethical issues [8]. Therefore, a computer simulation offers a possibility for studying the design, testing and validating the closed-loop system in silico. This simulation of a virtual patient could reduce the time, cost and burden for patients participating in the clinical studies. This preclinical testing can result in a direction for the clinical studies and shows beforehand the (in)effective control scenarios in a safe and cost effective manner.

1.4 Review of existing models

Two recent review articles describe the main existing simulation models for testing glucose controllers. These are the review of Wilinska et al. and the review of Colmegna et al. [11, 38]. The first review compares five models and the second review compares three models which are also mentioned in the first review. In total, five simulation models are compared: the Sorensen model, the Universities of Virginia and Padova (UVA/Padova) research group model, the University of Cambridge model, the Medtronic model and the model of Fabietti et al. These models simulate the glucose regulation of a diabetes patient. The models are used to investigate and design a closed-loop controller. These reviews describe the submodels of each model and discuss the simplifications, the assumptions and differences that are made.

The Sorensen model is an explanatory physiological model of the glucose metabolism. The model represents the organs in six compartments. These compartments are again divided in three spaces: the capillaries, the interstitial and the intracellular space. In these spaces the interactions of glucose, insulin and glucagon are described. These are represented as a mass balance. This model was the first complete model that simulates an average patient with type 1 diabetes. However, it simulates intravenous administrated insulin. Therefore, the delay when insulin is infused subcutaneously is neglected.

The UVA/Padova model exists of two subsystems, namely the glucose and insulin system. In a later publication an additional glucagon subsystem is presented. The

glucose subsystem is divided into three systems, which describe the transport, production and utilization of glucose. This model includes the subcutaneous insulin kinetics to simulate the administered insulin. The simulation population consists of 300 virtual patients including adults, adolescents and children. The model is approved by the Food and Drug Administration to replace animal trials.

The Cambridge's model consist of five submodels: the glucose and insulin kinetics, the glucose absorption, the subcutaneous insulin, and the interstitial glucose. Additionally, this research group included physical exercise to the model. With these extended submodels the model is specifically build to support the development of a closed-loop system. The model population consists of 18 virtual patients. The model is validated with an overnight clinical study.

The Medtronic and Fabietii models are based on the Bergman's minimal model from 1970, which is the most widely studied model [1, 33]. This model describes the interaction between the blood glucose concentration and the insulin concentration in blood [33]. The submodels of the glucose kinetics are simplistically represented using Bergman's model.

Comparing all these reviewed models, the Cambridge and UVA/Padova models are considered the most complete models for testing an AP. Both models are based on clinical data sets instead of literature. The differences between the models are seen in the compartmental structures. The main differences are the insulin absorption in the blood plasma after subcutaneous administration and the rate of appearance of intake of carbohydrates. These assumptions have an effect on the total number of compartments and therefore the amount of differential equations. More compartments make the model more complex. Which model is more suitable for testing an AP depends on the testing specifications.

1.5 Requirements

The AP of Inreda diabetic BV is designed by the company itself and includes pumps for insulin and glucagon administration, control algorithms and CGM. Eventually the medical device need to be tested in vivo, but in silico testing is easier and timesaving. In silico testing requires insight in physiologic systems of glucose control and the parameters of the AP's algorithm. Further, this simulation has to demonstrate the effect of changes made in the algorithm. As said, in silico testing requires a model that simulates the physiologic systems of glucose control: the glucose, insulin and glucagon kinetics and dynamics. Kinetics describe the reaction of the body to the substrate using the concentrations in the body fluids and tissue which vary over

time and in intensity of the response. Dynamics describe the substrates effect to the body and the different mechanisms by which the substrate acts. In glucose kinetics, it is important to distinguish the blood plasma and the interstitial space kinetics of glucose for the sensors. The CGM's measure glucose subcutaneously in the interstitial space. Furthermore, the liver has a major influence on the glucose dynamics. The liver affects the blood plasma glucose positively and negatively. Therefore, the liver has to be considered in the model. In addition, the utilization of glucose during physical activity is also essential for the glucose dynamics and are part of the simulation. Next, the absorption by the gastrointestinal(GI) tract after carbohydrate intake has to be included in the model.

Insulin and glucagon kinetics and dynamics are two important physiological systems. Insulin is administrated subcutaneously and therefore the absorption of insulin and peak activity is delayed compared to the normal insulin release of the pancreas. Therefore, the pharmacokinetics and pharmacodynamics of insulin need to be considered. Glucagon is also administrated subcutaneously, which should be considered in the model. Another requirement is the possibility to change parameters and to create inter-patients differences like insulin sensitivity.

1.6 Purpose

To provide insight in the human glucose regulation, several existing models are reviewed, each having their own strengths and limitations. The UVA/Padova and the Cambridge model are considered the most complete models for testing the AP. In both models the glucogon subsystem is not included. In an extension of the UVA/Padova model the glucagon subsystem is added [15]. This model part is based on non-published assumptions and it remains to be seen whether this part of the model is accurate. The insulin effect on the glucagon response in this study remains unclear. The study of Blauw et al. shows the pharmacokinetics and pharmacodynamics of various glucagon dosages at different blood glucose levels [3]. This study measured the glucagon kinetics and dynamics without the effect of insulin. This gives the opportunity to model the glucagon submodel according to these clinical data, providing the information to estimate the parameters for the glucagon part without the effect of insulin. Developing a proprietary model provides more insight in the human glucose regulation and a glucagon subsystem can be added to glucose regulation in the model.

The purpose of this thesis is to design a simulation model of patients with Type 1 Diabetes Mellitus (T1DM) suitable for testing the AP's algorithm of Inreda Diabetic BV. This provides more insight in the human glucose regulation and a proprietary model is easier to verify and control than the existing models.

2 Model development

In this study a model was designed to test the algorithm of the artificial pancreas. Figure 2.1 schematically gives an overview of the closed-loop system. It represents a common control system, in which the controller, the sensor and the process are connected and form the closed-loop system. In case of the AP, the controller represents the algorithm, the sensor consists of continuous glucose sensors and the process is the (virtual) patient. The controller delivers an amount of either insulin or glucagon to the virtual patient. The virtual patient is susceptible to disturbances from outside the system, like the intake of carbohydrates.

The process has 2 outputs: the plasma glucose concentration and subcutaneous glucose concentration. The plasma glucose value was only used as a control parameter, not as feedback loop. Plasma glucose level is a commonly used expression for the glucose value of the body. The CGM sensors measure the subcutaneous glucose value provided by the process and calculate the change of glucose, i.e. the slope. The glucose value and slope are sent to the algorithm that calculate the amount of administrated insulin or glucagon. This study focused on modeling the virtual patient.

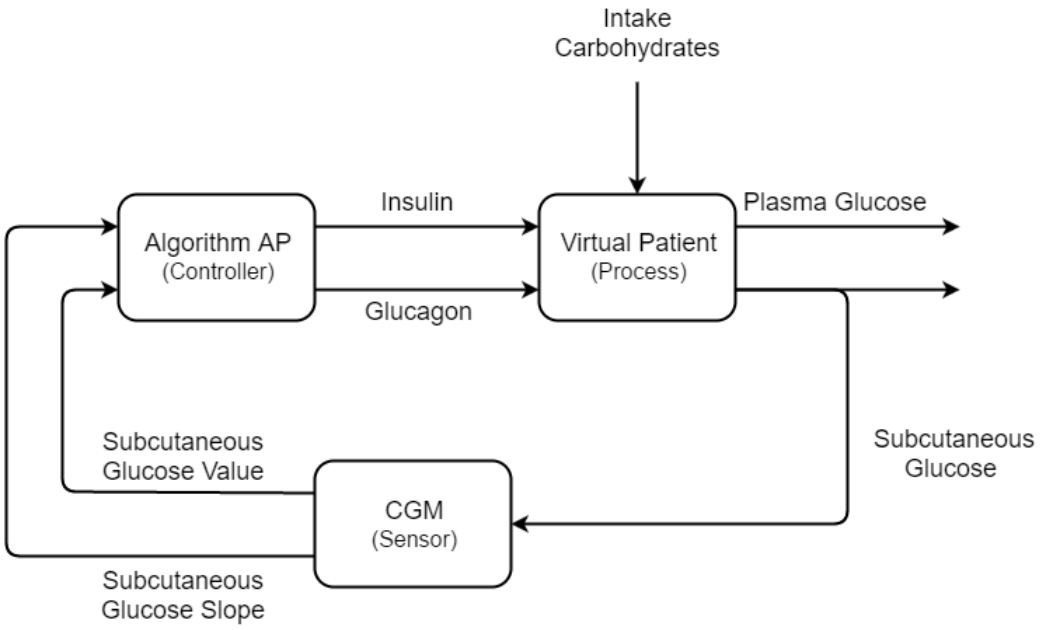

Figure 2.1: *Overview of the closed loop system with the AP's algorithm as controller, the virtual patient as process and the CMG as sensor.*

The virtual patient represents the glucose regulation system in T1DM patients. To simulate the glucose regulation, glucose, insulin and glucagon dynamics are represented in the model. These dynamics are the three main physiological subsystems that are modeled. Numbers in the upper right corner of the boxes in Figure 2.2 indicates these subsystems. The boxes with the number *1* are part of the glucose dynamics, number *2* represents part of insulin dynamics and the boxes with number *3* are part of the glucagon dynamics. Affix *a* describes absorption, transport and degradation of the three substrates. In box *1a* the plasma glucose and the subcutaneous glucose are described. These two glucose values are the subsystem outputs. Three boxes connect to this first subsystem indicated with the affixes *b*, *c* and *d*. These boxes describe the dynamics of endogenous glucose production (*1b*), the utilization of glucose (*1c*) and the glucose rate of appearance (*1d*). The pancreatic insulin and glucagon secretion are represented in boxes *2b* and *3b*. The boxes *2c* and *3c* describe the subcutaneous administration route of these hormones. The administrated insulin and glucagon provided by the AP enter the system i.e. the virtual patient by these two boxes. The arrows indicate the fluxes between the subsystems. The dotted arrows indicate the signals that influence the subsystems.

2.1 Glucose

Box 1a First the glucose kinetics are modeled, in box *1a* of Figure 2.2. Glucose concentrations fluctuate during the day. The amount of glucose increases and decreases respectively by intake of carbohydrates and utilization by the body. Glucose enters the body by the intake of food as carbohydrates. Eating food that contains carbohydrates increases the glucose in the blood plasma. Glucose is a major source of fuel for the body; the body organs need glucose to function. This utilization by the body is explained in detail in section 2.1.2. The body stores glucose that is not directly required. This storage happens in the liver and is released in fasting to increase the plasma glucose. The contribution of the liver to the glucose regulation is described in detail in section 2.1.1.

The changes in glucose concentration do not only occur in the blood plasma, but also in tissues and the interstitial space. The absorption of glucose is not directly from the blood plasma, but by a diffusion gradient. The tissues cells absorb the glucose through facilitated diffusion from this space. Box *1a* consists of both the glucose plasma and the interstitial glucose. Dividing these two spaces was also important for the sensor application in the closed loop system of Figure 2.1. The changes in the subcutaneous glucose concentration is measured with CGM sensors and is necessary for modeling.

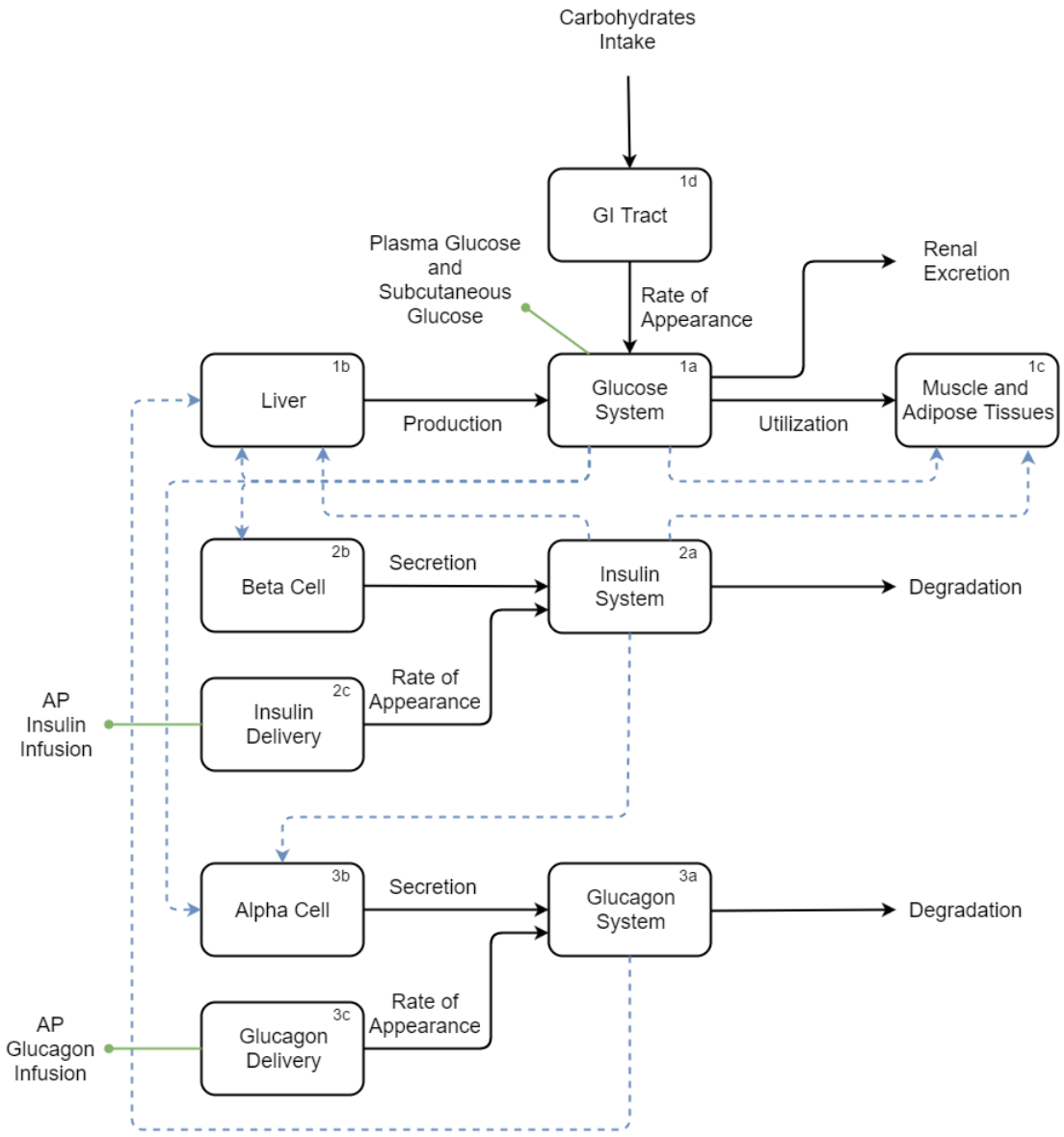

Figure 2.2: *The specification of the virtual patient. The boxes indicated with 1 are part of the glucose dynamics. The boxes with 2 are part of the insulin dynamics and the boxes with 3 are part of the glucagon dynamics. The green lines which end in a point indicate the interaction with the closed-loop system. The AP infusion points are indicated, this is the input for the virtual patients provided by the AP. The plasma glucose and subcutaneous glucose are the output of the virtual patient.*

In conclusion, box *1a* is modeled as a two compartment model [13, 39]. The first compartment describes glucose mass changes in the plasma. The second compartment describes the glucose mass changes in the interstitial space. Between these compartments the transport of glucose takes place by diffusion, therefore the assumption is that the compartment volumes are constant. The conversion from mass to concentration is made at the end of the modeling.

The two compartments are presented in Figure 2.3. This figure shows the inputs and outputs as discussed above. The glucose rate of appearance (Ra) from digested food and the endogenous glucose production (EGP) by the liver enter the left compartment. In this compartment the glucose diffuses to organs that can take up glucose without the use of insulin (insulin independent utilization, U_{ii}). The renal excretion of glucose is modeled as variable E. Renal excretion occurs if the plasma glucose levels reaches a certain threshold. The kidneys filter glucose and reabsorbs it to prevent lost. If the threshold is reached the reabsorption is limited and the glucose will be excreted with the urine. Glucose leaves to insulin dependent organs from the second compartment (U_{id}).

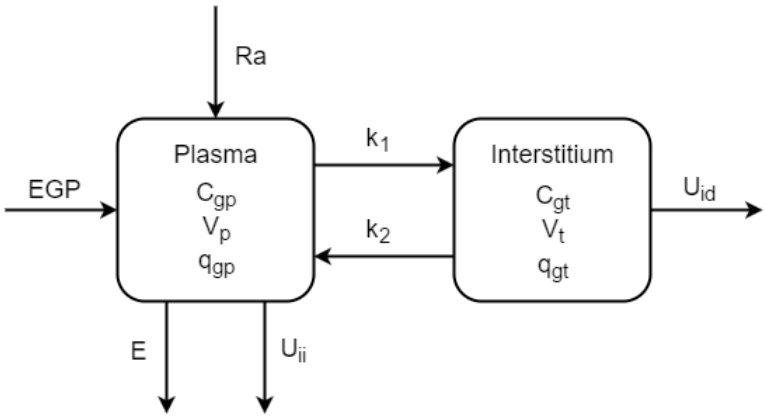

Figure 2.3: *The two compartment model for glucose kinetics of box 1a.*

Figure 2.3 helps to formulate the differential equations. The glucose mass in the compartments were used as quantities. The change in mass was determined by the input and output of glucose. These changes over time were expressed for both plasma and interstitial space as $q_{gp}(t)$ and $q_{gt}(t)$ respectively. This resulted in the following differential equations:

$$\begin{cases} \dot{q}_{gp}(t) = EGP(t) + Ra(t) - U_{ii}(t) - k_1 q_{gp}(t) + k_2 q_{gt}(t) & \text{(2.1a)} \\ \dot{q}_{gt}(t) = -U_{id}(t) + k_1 q_{gp}(t) - k_2 q_{gt}(t). & \text{(2.1b)} \end{cases}$$

Each equation describes the glucose dynamics in the blood plasma compartment Eq. (2.1a) and interstitial space compartment Eq. (2.1b). The rate parameters k_1 and k_2 in both equations determine the velocity of glucose exchange between the compartments.

2.1.1 Endogenous Glucose Production

Box 1b The liver plays an important role in the glucose regulation. At high levels of glucose plasma it stores glucose and at low levels of plasma glucose it releases glucose. The liver is both a source and a sink for glucose. After the intake of food, the liver stores the glucose absorbed by the gastrointestinal tract as glycogen. If there is no intake of carbohydrates, for example during a night sleep, the liver releases glucose from glycogen. The storage is stimulated by the hormone insulin. This hormone is released by the pancreas in response to high levels of blood glucose. This storage process is called glycogenesis. The hormone glucagon is released by the pancreas during low levels of blood glucose. Glucagon stimulates the liver to breakdown the glycogen into glucose. The glucose is subsequently released by the liver into the blood plasma. The breakdown process of glycogen is called glycogenolysis. Figure 2.4 shows the two processes schematically.

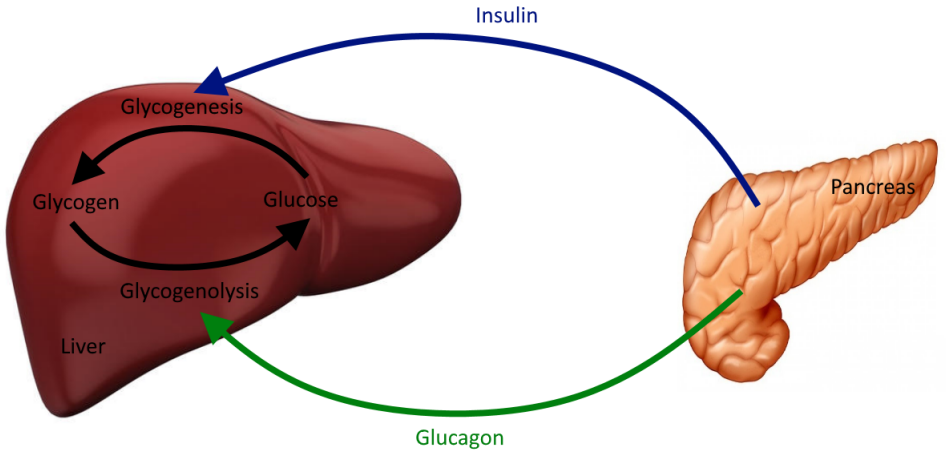

Figure 2.4: *The left organ is the liver, where the conversion from glucose to glycogen and the other way around occurs. The pancreas is presented on the right. This is the organ that releases the hormones insulin and glucagon. The insulin stimulates glycogen formation and the glucagon stimulates the breakdown of glycogen.*

Both glycogenesis and glycogenolysis affect the amount of glucose that passes the liver. The net result of these processes is the hepatic glucose production or EGP. Glycogenesis decreases the EGP, whereas glycogenolysis increases it. EGP is the result of the glucose regulation by the liver, and depends on the glucose mass in the plasma. The level of glucose determines the secretion of certain hormones by the pancreas. Insulin is secreted during hyperglycemia and stimulates the glycogenesis. Glucagon is secreted during hypoglycemia and stimulates glycogenolysis, subsequently the EGP. Besides these two liver processes, the liver is able to auto-regulate these processes. This auto-regulation is controlled by the glucose mass in the plasma. Hyperglycemia inhibits the rate of glycogenolysis, which is a negative feedback regulation [24, 27].

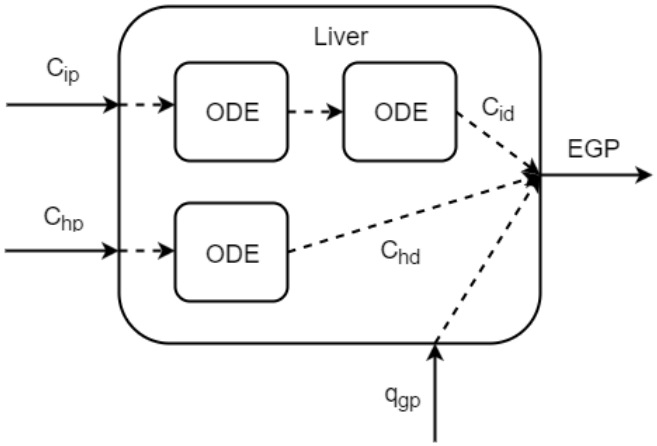

Figure 2.5: *A compartment overview of the EGP regulation. There are three inputs into the liver which influences the EGP. The plasma insulin concentration (C_{ip}), the plasma glucagon concentration (C_{hp}) and the plasma glucose mass (q_{gp}). The C_{ip} follows the route where it passes twice an ODE. The C_{hp} passes once an ODE and the q_{gp} has a direct effect on the EGP.*

Figure 2.5 is an overview of the model for EGP. It shows three inputs for this part of the system. Namely, the plasma insulin concentration ($C_{ip}(t)$), the plasma glucagon concentration ($C_{hp}(t)$) and the plasma glucose mass ($q_{gp}(t)$). $C_{ip}(t)$ follows the route where it is differentiated twice. The $C_{hp}(t)$ is once differentiated and the $q_{gp}(t)$ has a direct effect on the EGP.

The ordinary differential equations (ODEs) in Figure 2.5 cause a smooth reaction of the liver to the changes in hormone concentrations. The reaction is not immediately after a change of concentration. Eqs. (2.2a), (2.2b) and (2.2c) describe the reaction of the liver to the changes in hormone concentrations. An immediate response to a change is physiologically impossible. The insulin concentration in blood plasma ($C_{ip}(t)$) either increases or decreases. If the insulin increases, it still needs to reach the site of action, which is in this case the liver. These kinetics are represented by the ODEs and described by Eq. (2.2a) and Eq. (2.2b). This is in accordance with the study of Dalla Man et al. This study describes the insulin action on the liver by two differential equations, which seemed to be the best fit to describe the clinical data. A possible explanation can be that first, the insulin has to diffuse from the portal vein to the interstitial space of the liver tissue. And secondly, it has to bind to certain receptors located at the cell membranes. The parameter k_{id} is a rate parameter and determine the time between the insulin signal and the insulin action on the liver. The interaction of glucagon with the liver is represented with one differential equation. The glucagon concentration ($C_{hd}(t)$) passes one ODE in Figure 2.5 and is described by Eq. (2.2c). This is the hepatic reaction to glucagon. The reaction of the liver is stronger when it crosses the basal value ($C_{hp,b}$). The parameter k_{hd} is

again a rate parameter and describe the time between the glucagon signal and the glucagon action on the liver.

$$\begin{cases} \dot{C}_x(t) = -k_{id}(C_x(t) - C_{ip}(t)) & \text{(2.2a)} \\ \dot{C}_{id}(t) = -k_{id}(C_{id}(t) - C_x(t)) & \text{(2.2b)} \\ \dot{C}_{hd}(t) = -k_{hd}C_{hd}(t) + k_{hd}\max[(C_{hp}(t) - C_{hp,b}), 0] & \text{(2.2c)} \end{cases}$$

The $C_{id}(t)$ of Eq. (2.2b) and the $C_{hd}(t)$ in Eq. (2.2c) together with the $q_{gp}(t)$ affect the $EGP(t)$. This is described by

$$EGP(t) = EGP_0 - k_{ge}q_{gp}(t) - k_{il}C_{id}(t) + k_{hl}C_{hd}(t) \tag{2.3}$$

and represents the changes as a result of the liver processes. In Eq. (2.3), EGP_0 is the constant release of EGP. The other terms in Eq. (2.3) are negatively or positively affecting the total EGP as function of time. $k_{ge}q_{gp}(t)$ is the inhibition of glucose on EGP. More specifically, the inhibition of glycogenolysis. The parameter k_{ge} represents the reaction strength of glucose on the liver, or liver glucose effectiveness. $k_{il}C_{id}(t)$ describes the hepatic insulin sensitivity, where the parameter k_{il} is the hepatic responsivity of insulin. This describes the storage of glucose by the glycogenesis process. $k_{hl}C_{hd}(t)$ in Eq. (2.3) represents the stimulation of EGP by glucagon, which is the stimulation of the glycogenolysis process. The k_{hl} is the hepatic responsivity to glucagon.

Eq. (2.3) describes the changes in the EGP, which is a reflection of the glucose processes in the liver described by Figure 2.4. However, this is not the only glucose metabolic process that occurs in the liver. The stored glycogen can be exhausted if glycogen is not supplemented by glycogenesis. This happens when fasting is prolonged. In that situation, the source of available glucose changes, it is constructed from the breakdown of proteins. This process is called gluconeogenesis and is auto regulated by the liver instead of by hormones. Hypoglycemia stimulates the rate of gluconeogenesis when the glycogen reserves are depleted. This process is important to maintain the blood glucose level. In this model, the gluconeogenesis is not modeled as it is assumed that the patient in the model does not have prolonged hypoglycemia. Therefore, gluconeogenesis is omitted from the model.

2.1.2 Glucose utilization

Box 1c Glucose is one of the sources for energy in the body. The utilization of glucose occurs in the cells of the organs via the interstitial space. The glucose absorption into the cells is facilitated by membrane transporter proteins, so called GLUT proteins. This transport is either insulin dependent or insulin independent. The

insulin dependent transport occurs in cells where GLUT-4 transporters are present. Insulin works as a key to open the locked cells in order to store the glucose. The GLUT-4 transporters are mainly found in adipocytes and myocytes. The transporters are not always present on the cell membrane. During euglycemia the GLUT-4 transporters are concealed in vesicles inside the cell, about 90% of the transporters are concealed in this manner [31]. This means that relatively few transporters are active on the surface of the cell. Hence, the transport of glucose is kept at a low speed.

During hyperglycemia insulin is secreted in the blood plasma. Insulin binds to its receptor on the cell surface. This activates the migration of the GLUT-4 transporter. The vesicle with the GLUT-4 transporter migrates from inside the cell to the cell membrane. Exocytosis allows the transporter to facilitate the glucose. Exocytosis is the fusion of the vesicle with the membrane of the cell. The mechanism of the glucose uptake by the GLUT-4 transporter is shown in Figure 2.6.

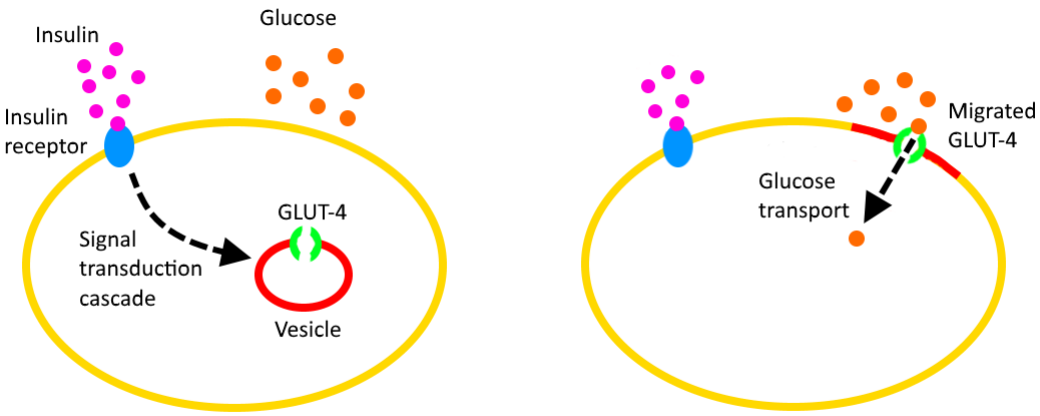

Figure 2.6: *On the left side the insulin binds to the insulin receptor. This activates the signal transduction cascade. The cascade provides the vesicle with the GLUT-4 transporter to migrate to the cell membrane. On the right side the vesicle fused with the cell membrane, the exocytosis. GLUT-4 transports the glucose from outside the cell to inside the cell.*

Figure 2.6 shows an example of a transporter that migrates to the cell membrane. As long as the insulin concentration is high, more vesicles migrate to the membrane. This increases the transport capability of the cell, and subsequently an increase in glucose transportation. It is assumed that the glucose transport is limited to the rate of glucose utilization. This transport is included in the model. Furthermore, the adipocytes and myocytes were assumed to have the same behavior in this part of the model. Both cells use the GLUT-4 transporters for the purpose of glucose absorption. The difference between the cells is the storage of glucose. Adipocytes convert glucose to triglycerides, where myocytes store glucose as glycogen.

A consequence of the assumption that adipocytes and myocytes are the same cell

types, is that the effect of physical activity is not present in the model. Physical activity augment GLUT-4 transporters in myocytes [23, 29]. The translocation and transcription increase by frequently exercise. The effect of muscle contraction, which stimulates migration of GLUT-4 transporters as well, is also ignored in this model.

In conclusion, the facilitated GLUT-4 glucose transport is mediated by insulin. This influences the rate of glucose absorption by the cells. The Michaelis-Menten equation is commonly used to describe this phenomenon. This equation describes how the velocity of an enzymatic reaction depends on the substrate concentration. The enzymatic reaction is the binding of glucose to the GLUT-4 transporter, with glucose as the substrate. A higher concentration of extracellular glucose increases the transport velocity. The velocity is also depending on the insulin concentration. The total glucose utilization is represented by:

$$U(t) = F + \frac{V_{m0} + V_{mcii} C_{ii}(t) q_{gt}(t)}{K_{m0} + q_{gt}(t)}. \tag{2.4}$$

The fraction in the equation is the Michaelis-Menten representation. V_{m0} is the maximal glucose absorption rate at the maximal level of glucose and K_{m0} is Michaelis-Menten's constant at which the glucose utilization is half the V_{m0} at the basal level of insulin. The Michaelis-Menten's constant expresses the affinity to bind glucose to the transporter. The lower the value, the higher the affinity for glucose. $q_{gt}(t)$ is the amount of glucose in the interstitial space. F is the glucose utilization of the central nervous system and the erythrocytes, the red blood cells. The term $V_{mcii} C_{ii}(t)$ is the influence of insulin on the transport sites, where $C_{ii}(t)$ is the insulin concentration in the interstitial space. This concentration depends on the insulin concentration of the blood glucose plasma. Furthermore, the insulin bound to its receptor on the cell membrane is utilized. The insulin concentration in the interstitial space was described by:

$$\dot{C}_{ii}(t) = -p C_{ii}(t) + p(C_{ip}(t) - C_{ip,b}). \tag{2.5}$$

The minus p parameter describes the uptake of insulin by the cells. The plus parameter p represent the diffusion of insulin from the blood to the interstitial space. This diffusion occurs when the plasma insulin concentration ($C_{ip}(t)$) is higher than the basal level ($C_{ip,b}$).

2.2 Insulin

Box 2a Insulin is a hormone secreted by the pancreas during hyperglycemia. The insulin effect is to lower the glucose levels. It facilitates glucose transport in cells, as explained in the previous section 2.1.2. In a healthy person, insulin is secreted in the splenic vein by the pancreatic β-cells during hyperglycemia. This vein drains

into the portal venous system of the liver and thereafter in the systemic circulation and body. The anatomical representation is shown in Figure 2.7. The consequence of the anatomical location of the liver and the pancreas is the insulin extraction by the liver. Not all the secreted insulin will reach the rest of the body. A part of the secretion is cleared by the liver and a part stimulates glycogenesis, as discussed in the section 2.1.1. The liver is responsible for the breakdown and excretion of insulin. The liver regulates the insulin extraction, which results in the regulation of glucose. The insulin regulation by the liver is important to include in the model.

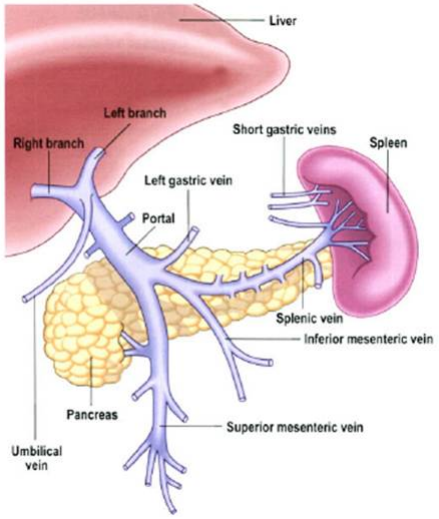

Figure 2.7: *The anatomical representation of the organs: liver, pancreas and spleen. Further the veins of the organs are shown. This shows that the splenic vein flows into the portal vein. The portal vein flows to the liver.*

The insulin is described by a two compartment model, shown in Figure 2.8. The compartments describe the insulin dynamics in the liver and plasma. The first compartment represents the liver and the second compartment the plasma. In the liver compartment the insulin extraction is presented by the arrow m_3. The arrow m_4 is the insulin excretion that occurs in the plasma. This is the insulin extraction by the kidneys.

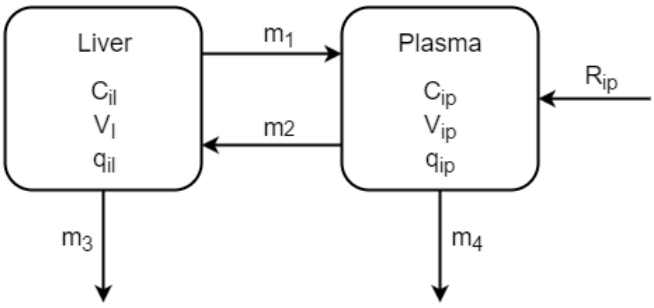

Figure 2.8: *The two compartment model for insulin.*

The insulin model is described by the differential equations:

$$\begin{cases} \dot{q}_{il}(t) = -(m_1 + m_3(t))q_{il}(t) + m_2 q_{ip}(t) & \text{(2.6a)} \\ \dot{q}_{ip}(t) = m_1 q_{il}(t) - (m_2 + m_4)q_{ip}(t) + R_{ip}(t). & \text{(2.6b)} \end{cases}$$

Eqs. (2.6a) and (2.6b) describe the insulin dynamics of the two compartments. The first compartment was presented by Eq. (2.6a) and describes the insulin mass in the liver ($q_{il}(t)$). In these equations the rate parameters (m_1,m_2) represent the exchange between the two compartments. The second compartment describes the insulin mass in the blood plasma ($q_{ip}(t)$). In this compartment the subcutaneously administered insulin (R_{ip}) is entering this part of the system. $m_3(t)$ is the insulin extraction by the liver and is described by:

$$m_3(t) = \frac{HE(t)m_1}{1 - HE(t)}. \tag{2.7}$$

$HE(t)$ in Eq. (2.7) is the hepatic extraction. This is a time varying parameter. More insulin is secreted during hyperglycemia, because the insulin is needed by the body and hence the liver will excrete more insulin. This is described by Eq. (2.7). The hepatic extraction of the insulin is described by:

$$HE(t) = -m_5 S_i(t) + m_6. \tag{2.8}$$

In Eq. (2.8) the study of Meier et al. was followed [26]. That study indicates that the insulin secretion $S_i(t)$ linearly correlates with the hepatic extraction. The parameter m_5 determined the amount of secreted insulin that is extracted by the liver. Parameter m_6 is the amount of insulin that passes the liver. Substituting Eq. (2.8) in Eq. (2.7) gives

$$m_3(t) = \frac{(-m_5 S_i(t) + m_6)m_1}{1 - (-m_5 S_i(t) + m_6)}. \tag{2.9}$$

Eq. (2.9) describes the amount of insulin extraction from the blood. The equation shows that if the insulin secretion increases, the proportion of insulin extraction by the liver is less. More insulin will pass the liver and enter the systemic circulation. During hyperglycemia more insulin reaches the body organs and subsequently more glucose is utilized and the plasma glucose returns to euglycemia.

The second compartment in Figure (2.8) describes the plasma insulin and is presented by Eq. (2.6b). Again both rate parameters (m_1,m_2) are present. The parameter (m_4) describes the insulin clearance from the plasma.

Eq. (2.9) describes the situation for a healthy person. The secreted insulin enters the liver compartment. Only, in a T1DM patient the pancreatic β-cells are dysfunctional. The insulin enters the model as a subcutaneous administration. This

is explained in the next section 2.2.1. The insulin input appears in the second compartment and is shown in Eq. (2.6b) with the term (R_{ip}). Insulin follows a different route compared to a healthy person. It enters the blood circulation after the subcutaneously administration. The physiological first-pass effect is bypassed. The first-pass effect is the effect of the extraction of, in this case, the hormone by the liver. The concentration that enters the liver is lower for the subcutaneous administered insulin and, therefore, the liver extraction is lower. This changes Eq. (2.9), because the secretion ($S_i(t)$) is not present in T1DM patients. For the model this was changed to the amount of insulin in the plasma ($q_{ip}(t)$). The equation for $m_3(t)$ becomes now:

$$m_3(t) = \frac{(-m_5 q_{ip}(t) + m_6)m_1}{1 - (-m_5 q_{ip}(t) + m_6)}. \tag{2.10}$$

2.2.1 Insulin administration

Box 2c In T1DM patients the β-cell is destroyed and the patients are dependent of exogenous insulin that is administered subcutaneously. This insulin is a synthetic recombinant insulin. Most of this short acting insulin is a polymer build up from multiple monomers with substrates to conserve the fluid. A small part is dimer because of the immediately effect of the short acting insulin. If administered, the insulin degrades to dimers. The dimers diffuse to the blood plasma. This subcutaneously administered insulin consist of polymers and dimers and therefore a three-compartment model is built, Figure 2.9. The first compartment is the depot of the polymer insulin and the second compartment represents the depot of the dimers, the third compartment is the plasma.

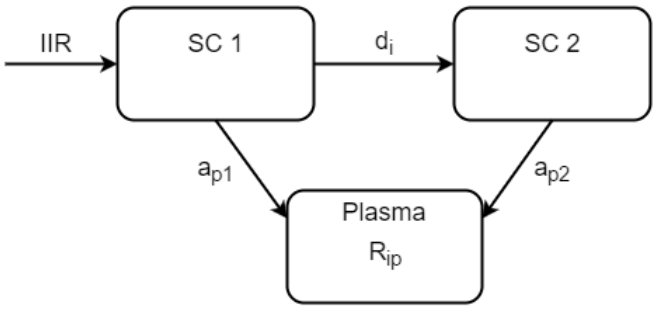

Figure 2.9: *The representation of the subcutaneous administration route of insulin.*

The subcutaneous administration is described by three equations:

$$\begin{cases} \dot{q}_{Isc1}(t) = IIR(t) - a_{p1} q_{Isc1}(t) - d_i q_{Isc1}^{\frac{2}{3}}(t) & \text{(2.11a)} \\ \dot{q}_{Isc2}(t) = d_i q_{Isc1}^{\frac{2}{3}} - a_{p2} q_{Isc2} & \text{(2.11b)} \\ R_{ip}(t) = a_{p1} q_{Isc1}(t) + a_{p2} q_{Isc2}. & \text{(2.11c)} \end{cases}$$

Eqs. (2.11a) and (2.11b) describe the absorption of the administered insulin. $\dot{q}_{Isc1}(t)$ in Eq. (2.11a) represents the compartment with the polymers. $\dot{q}_{Isc2}(t)$ is the compartment with the dimers represented by Eq. (2.11b). It is assumed that the injected fluid forms a sphere at the subcutaneous site and that the absorption starts at the surface of the sphere. The decreasing volume of the sphere is described with a power of $\frac{2}{3}$. Insulin absorption in the plasma ($R_{ip}(t)$) is represented by Eq. (2.11c).

2.3 Glucagon

Box 3b Glucagon is secreted by α- cells when the glucose level is low and counteracts the effect of insulin. Glucagon is secreted into the splenic vein. The splenic vein ends up in the portal vein of the liver. The anatomical proximity of the pancreas and liver is advantageous for glucagon's desired effects. The liver is the main target organ for glucagon. Glucagon regulates the hepatic metabolism of glycogen. It stimulates the liver to release glucose into the circulation by glycogenolysis and gluconeogenesis.

The glucagon concentration in the blood plasma increases by the secretion rate of α-cells. The glucagon concentration decreases by the transport between the plasma and interstitial space. The equilibrium of glucagon is very fast due to its extremely rapid kinetics [16]. The changes in glucagon plasma concentration is described by:

$$\dot{C}_{hp}(t) = -nC_{hp}(t) + S_h(t) + R_{hp}(t). \tag{2.12}$$

The glucagon removal in the plasma is determined by the rate parameter n. $nC_{hp}(t)$ represents the decreasing term of the glucagon concentration in Eq. (2.12). The $S_h(t)$ is the secreted glucagon by the pancreatic α-cells. The glucagon secretion is explained in the next section 2.3.1. The glucagon concentration is also increased by the subcutaneously administered glucagon $R_{hp}(t)$. This is explained in section 2.3.2.

2.3.1 Glucagon secretion

Box 3b During hypoglycemia the α-cells sense the low glucose level in blood plasma. A signal enters the cell through the GLUT-2 transporter, which activates the K_{ATP} channel to actively transport potassium ions. This depolarizes the membrane potential, establishing a less negative potential across the cell membrane. This results in an influx of sodium ions and influx of calcium ions. The increase of calcium activates the glucagon release. This process is shown in Figure 2.10. The glucagon

secretion depends on the depolarization of the α-cell membrane. In the opposite case, the hyperpolarization of the cell membrane reduces the glucagon release. For higher glucose concentration there is no signal given by the GLUT-2 transporter, which prevents the K_{ATP} channel to excrete potassium. The intracellular concentration becomes more negative, reducing the glucagon release.

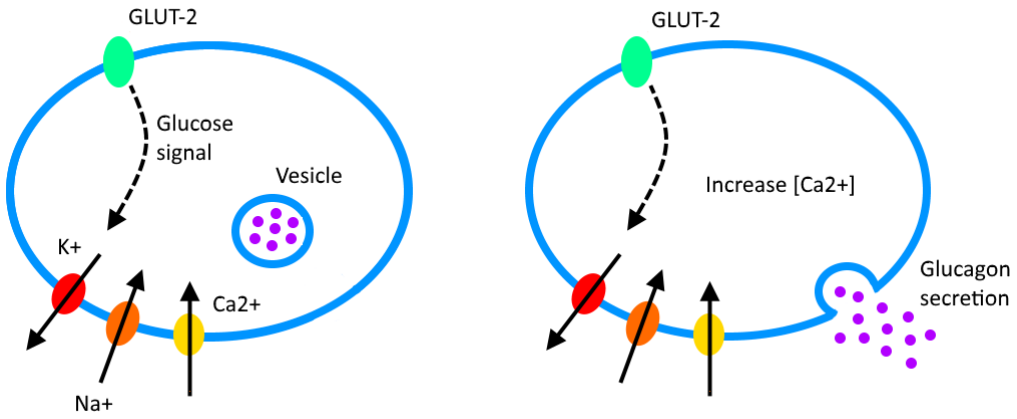

Figure 2.10: *The action potential of the alpha cell and secretion pathway of glucagon. During low levels of glucose the alpha cell senses this and allows K_{ATP} to secrete K^+, this depolarizes the cell. Na^+ enters the cell, followed by Ca^{2+}. The calcium activates the secretion of glucagon. The release of glucagon happens pulsatile.*

Glucagon secretion follows an episodic secretion. This pattern is described by two phases, the static and dynamic phase. The two phase secretion is represented by the equations:

$$\begin{cases} \dot{S}_{h,static}(t) = -\rho[S_{h,static}(t) - \max[\sigma(h - C_{gp}(t)) + S_{h,b}, 0)] & \text{(2.13a)} \\ S_{h,dynamic}(t) = \delta \max[-\dot{C}_{gp}(t), 0] & \text{(2.13b)} \\ S_h(t) = S_{h,static}(t) + S_{h,dynamic}(t). & \text{(2.13c)} \end{cases}$$

If the glucose concentration gets below a certain glucose level, glucagon is secreted. This moment is indicated in Eq. (2.13a) by $[h - C_{gp}(t)]$, where h is the threshold. This applies for the static part. Parameter ρ is the rate parameter for the static release. σ is the α- cell responsivity to the glucose level in the plasma. The static part was limited by the max function. If the condition $\sigma[h - C_{gp}(t)] + S_{h,b}$ is higher than zero, the condition contributes to the secretion, otherwise this part of the equation is zero. The $S_{h,b}$ is the basal glucagon secretion. The dynamic part described by Eq. (2.13b) depends on the decreasing rate of the plasma glucose concentration. δ is the rate parameter for the dynamic part. Again, this equation was limited by the max function. The total secretion is the addition of the static ($S_{h,static}(t)$) and dynamic secretion ($S_{h,dynamic}(t)$).

2.3.2 Glucagon administration

Box 3c The subcutaneous administration of glucagon is assumed to follow the same pathway as the subcutaneous administration of insulin. The study of Lv et al. indicates that a three-compartment model is the best way to describe glucagon dynamics of the subcutaneous route. The compartments are represented in Figure 2.11. Again, the assumption is made that the fluid forms a sphere once administered. This is in contrast to the study of Lv et al.

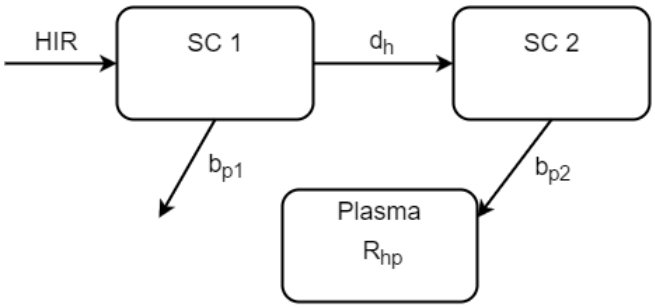

Figure 2.11: *Representation of the subcutaneous administration route of glucagon.*

The subcutaneous administration of glucagon is described by three equations:

$$\begin{cases} \dot{q}_{Hsc1}(t) = HIR(t) - b_{p1}q_{Hsc1}(t) - d_h q_{Hsc1}^{\frac{2}{3}}(t) & \text{(2.14a)} \\ \dot{q}_{Hsc2}(t) = d_h q_{Hsc1}^{\frac{2}{3}} - b_{p2}q_{Hsc2} & \text{(2.14b)} \\ R_{hp}(t) = b_{p1}q_{Hsc1}(t). & \text{(2.14c)} \end{cases}$$

Eqs. (2.14a) and (2.14b) describe the absorption of the subcutaneously administered glucagon. $\dot{q}_{Hsc1}(t)$ represents the changes of administered glucagon in the first compartment and $\dot{q}_{Hsc2}(t)$ the changes in the second compartment. The decrease in volume of glucagon is also described with a power of $\frac{2}{3}$. Glucagon absorption in the blood plasma ($R_{hp}(t)$) is represented by Eq. (2.14c). This is slightly different compared to insulin. The glucagon absorption in the plasma is only from the second compartment. In contrast to the insulin, where the absorption is from the first and the second compartment. The outflow from the first compartment is lost.

2.4 Model

A virtual patient is modeled by the submodels indicated in Figure 2.2. These submodels are explained in the previous sections, except for the GI tract. This is discussed in section 5.1. The submodels describe the three main physiological subsystem of the glucose regulation, the glucose, insulin and glucagon. The glucose

subsystem consists of 4 parts and the first 3 are modeled during this study by 8 mathematical equations. The insulin subsystem is divided into 3 parts and 2 are modeled in this study, because the β-cell part is assumed to be zero. 6 mathematical equation are used to describe the insulin subsystem. The glucagon subsystem consists of 3 parts and are all modeled in this study by 7 mathematical equation. In summary, the total model is divided into 10 parts as Figure 2.2 shows and exists of 14 differential equations and 7 mathematical equations. The model consists of 35 parameters that need to be estimated and calculates 28 output values. The parameters and outputs are listed in Table 2.1. The abbreviations used in the equations are explained by the quantity and the unity.

Table 2.1: *The outputs and parameters used in the model consisting of 21 equations. The abbreviations used in the equations are explained by the quantity and the unity.*

Abbreviation	Quantity	Unity
a_{p1}	Rate parameter subcutaneous insulin transport	min^{-1}
a_{p2}	Rate parameter subcutaneous insulin transport	min^{-1}
b_{p1}	Rate parameter subcutaneous glucagon transport	min^{-1}
b_{p2}	Rate parameter subcutaneous glucagon transport	min^{-1}
C_{hd}	Concentration of delayed glucagon in the interstitial space	ng/L
C_{hp}	Concentration of glucagon in the blood plasma	ng/L
$C_{hp,b}$	Concentration of basal glucagon in the blood plasma	ng/L
C_{id}	Concentration of delayed insulin in the interstitial space	$pmol/L$
C_{ii}	Concentration of insulin in the interstitial space	$pmol/L$
C_{ip}	Concentration of insulin in the blood plasma	$pmol/L$
$C_{ip,b}$	Concentration of basal insulin in the blood plasma	$pmol/L$
C_x	Concentration of insulin in the liver	$pmol/L$
d_h	Rate parameter absorption of subcutaneous glucagon	min^{-1}
d_i	Rate parameter absorption of subcutaneous insulin	min^{-1}
E	Excretion of glucose by the kidneys	$mg/kg/min$
EGP	Endogenous glucose production	$mg/kg/min$
EGP_0	Extrapolated EGP at zero glucose and insulin	$mg/kg/min$
F	Glucose absorption by the brain and erythrocytes	$mg/kg/min$
h	Glucose threshold level for glucagon secretion	mg/dL
HE	Hepatic Extraction of insulin	$dimensionless$
HIR	Glucagon infusion rate	$ng/kg/min$
IIR	Insulin infusion rate	$pmol/kg/min$
k_1	Rate parameter of glucose transport to the interstitial space	min^{-1}
k_2	Rate parameter of glucose transport to the blood plasma	min^{-1}
k_{ge}	Liver glucose effectiveness	min^{-1}
k_{hd}	Rate parameter between insulin signal and insulin action in the liver	min^{-1}

Table2.1 – continued from previous page

Abbreviation	Quantity	Unity
k_{hl}	Glucagon action on the liver	$mg/kg/min$ $per\ ng/L$
k_{id}	Delay parameter between insulin signal and insulin action	min^{-1}
k_{il}	Insulin action on the liver	$mg/kg/min$ $per\ pmol/L$
K_{m0}	Michaelis-Menten constant for GLUT-4	mg/kg
m_1	Rate parameter of insulin transport to the blood plasma	min^{-1}
m_2	Rate parameter of insulin transport to the interstitial space	min^{-1}
m_3	Rate parameter of insulin transport from the liver	min^{-1}
m_4	Rate parameter of insulin from the blood plasma	min^{-1}
m_5	Rate parameter of secreted insulin to the blood plasma	min^{-1}
m_6	Rate parameter of hepatic insulin extraction	min^{-1}
n	Rate parameter of glucagon from the blood plasma	min^{-1}
p	Rate parameter of insulin to the interstitial space	min^{-1}
q_{gp}	Mass of glucose in the blood plasma	mg/kg
q_{gt}	Mass of glucose in the interstitial space	mg/kg
q_{Hsc1}	Mass of glucagon in the subcutaneous space	ng/kg
q_{Hsc2}	Mass of glucagon in the subcutaneous space	ng/kg
q_{il}	Mass of insulin in the liver	$pmol/kg$
q_{ip}	Mass of insulin in the blood plasma	$pmol/kg$
q_{Isc1}	Mass of insulin in the subcutaneous space	$pmol/kg$
q_{Isc2}	Mass of insulin in the subcutaneous space	$pmol/kg$
Ra	Rate of appearance of glucose in the blood plasma after carbohydrate intake	$mg/kg/min$
R_{hp}	Rate of appearance of glucagon in the blood plasma	$ng/kg/min$
R_{ip}	Rate of appearance of insulin in the blood plasma	$pmol/kg/min$
S_h	Secretion of glucagon by the pancreatic alpha cells	$ng/kg/min$
$S_{h,dynamic}$	Secretion of dynamic phase of glucagon by the pancreatic alpha cells	$ng/kg/min$
$S_{h,static}$	Secretion of static phase of glucagon by the pancreatic alpha cells	$ng/kg/min$

Table2.1 – continued from previous page

Abbreviation	Quantity	Unity
$S_{h,b}$	Basal glucagon secretion by the pancreatic alpha cells	$ng/kg/min$
S_i	Secretion of insulin by the pancreatic beta cells	$pmol/kg/min$
U	Total utilization of glucose	$mg/kg/min$
U_{id}	Insulin dependent utilization of glucose	$mg/kg/min$
U_{ii}	Insulin independent utilization of glucose	$mg/kg/min$
V_{m0}	Maximal velocity of glucose	$mg/kg/min$
V_{mcii}	Maximal velocity of glucose transport dependent on insulin	$mg/kg/min$ $per\ pmol/L$
δ	Sensitivity parameter of the alpha cell to glucose	$ng/L \quad per$ mg/dL
ρ	Rate parameter of the glucagon secretion into the blood plasma	min^{-1}
σ	Alpha cell responsivity to glucose level	$ng/L/min$

3 Simulation

In chapter 2 the mathematical description of the model is described. The model is designed to simulate T1DM patients suitable for testing the AP's algorithm. It represents the glucose regulation system by describing the glucose, insulin and glucagon dynamics. These are the three subsystems and their interaction are modeled.

As mentioned before, the model reacts on the administered hormones received from the AP as an input. The model provides the simulated glucose values. The glucose values are the output of the model. These values are shown in a graph. Furthermore, it is interesting to monitor additional parameters to serve as valuable feedback for the researcher. Plasma insulin and glucagon concentration affect the EGP and glucose utilization, all of which influence the glucose concentration in the blood plasma. These four additional parameters are also plotted in graphs.

In this chapter an example is given of simulation result. Figure 3.1 shows the outputs of the simulation. For the simulation the values presented in the study of Dalla Man et al. are used. The parameter values for a healthy person are used because of the missing values of T1DM patients. A signal is reconstructed to simulate the glucose appearance in the blood plasma. This is the effect of the intake of a mixed meal containing $78\ g$ of glucose [13]. The model does not simulate the β-cell. Therefore, the insulin is simulated similar to the MDI therapy and thus provided by 1 subcutaneously insulin injection. This administration is also modeled as a short impulse to the system by $100\ units$ of insulin an equivalent to $3.5\ mg$ insulin.

Three simulations are performed. The first simulation is an example of a glucose input by a meal. The insulin is subcutaneous injected and at the same time the intake of carbohydrates is started. This is normal procedure for T1DM patients. When a T1DM patient eats, he or she should count the amount of carbohydrates before the meal. Patients have to inject a calculated amount of insulin corresponding to the amount of carbohydrates. Secondly, a simulation is performed of a patient who injected the same calculated amount of insulin, but administered it $30\ minutes$ after the start of the glucose appearance. This can occur if a patient forgets to inject the insulin in time. The third simulation represents an injection of insulin, while the patient did not eat in time and eats less carbohydrates than anticipated. The patient started eating $30\ minutes$ after the injected insulin and eat $39\ g$ of glucose,

which is half the meal. Therefore, the amount of administrated insulin is higher than required. This happens when something interrupts diner time and the patient eat less than expected. These three situation are represented in Figure 3.1. Where the blue line is simulation 1, the red dashed line is simulation 2 and the green dotted line is simulation 3.

Figure 3.1b is the input to the system, the glucose appearance in the blood plasma from a digested meal. It shows an impulse response that slowly decreases over the hours. Figure 3.1c shows the hepatic EGP. Figure 3.1d represents the insulin concentration in the blood plasma as a result of the subcutaneously administered insulin. Figure 3.1e presents the total utilization of glucose. Figure 3.1f shows the plasma glucagon. The glucagon is secreted by the α-cells in reaction to low plasma glucose levels. Glucagon is not subcutaneously administered in these simulations. The EGP and utilization influence the plasma glucose level and are affected by the hormones insulin and glucagon. Furthermore, each graph of Figure 3.1 shows the 3 simulated situations.

Looking at the first simulation. Figure 3.1a shows a peak in glucose concentration. The glucose plasma concentration returns to its steady state with a small fluctuation after $2\ hours$. A small increase is seen from 2 to $4\ hours$, after which it increases again. While glucose is still available up to $6\ hours$ after eating, see Figure 3.1b. The slightly elevated glucose concentration after the main peak starts at the same time as the EGP increases. The plasma insulin reaches a peak within an hour and disappears within $2\ hours$. Only, the effect of insulin is longer present. This is seen in Figure 3.1e. The peak of the glucose utilization starts at the same time as the plasma concentration peak of insulin. After $3\ hours$ the utilization is back to the basal state, which is longer than the present of insulin in the plasma. As soon as the glucose concentration decreases, the plasma glucagon increases. This is seen in Figure 3.1f, where at $1\ hour$ the increase in plasma glucagon is shown.

Next simulation 1 and 2 are compared with each other. In Figure 3.1 these situations are represented by the blue and red curves, respectively. The red curve in Figure 3.1a shows what happens with the plasma glucose, when the insulin injection is administered after a meal. The glucose concentration increases more than for simulation 1 and reaches a higher maximum. The administered insulin after the meal results in a later utilization peak. At the time the insulin concentration increases in the blood plasma and utilization increases at the same time as Figure 3.1e shows. Noticeable is that the utilization peak reaches a higher level for the same amount of insulin. This higher level is caused by the higher level of glucose concentration. Figure 3.1c shows that the suppression of EGP differs for the later administered insulin. The suppression is immediately present, this is caused by the increase of glucose. The higher glucose peak also decreases faster, this results in a

stronger glucagon reaction. Figure 3.1f shows this stronger increase in the glucagon concentration.

Finally the third situation is simulated. This is the situation where a smaller meal is taken at a later time. Figure 3.1a shows a decrease of glucose. This decrease is the effect of the administered insulin without intake of carbohydrates. The insulin in Figure 3.1d follows the same curve as in the first simulation. The reaction in glucose utilization starts at the same moment. Only, this time the utilization does not reach a level as high as for the first simulation. This is expected, since the glucose appearance is not present yet. Due to a decrease in glucose, the plasma glucagon increases. This effects the EGP, as is seen in Figure 3.1c. Contrary to simulations 1 and 2, the EGP increases. The higher EGP and glucose appearance both increase the glucose plasma concentration.

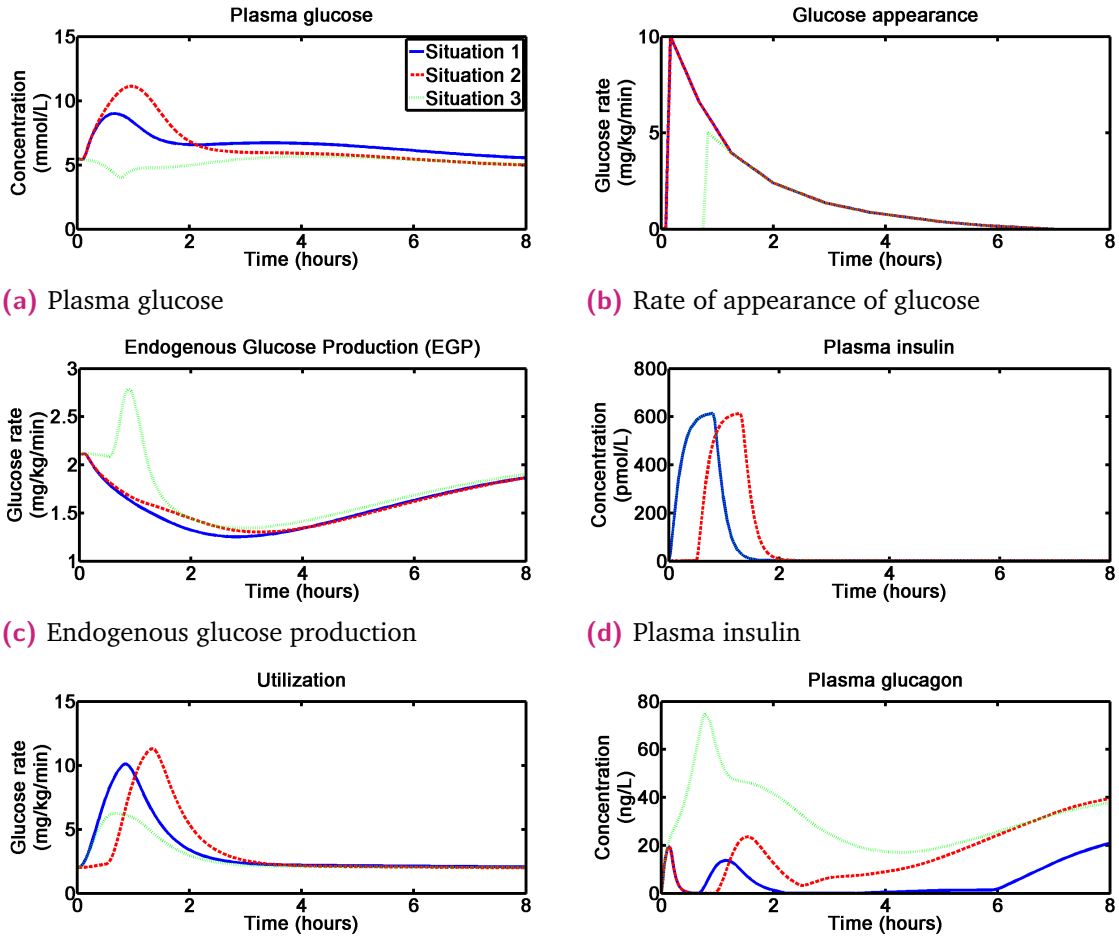

(a) Plasma glucose

(b) Rate of appearance of glucose

(c) Endogenous glucose production

(d) Plasma insulin

(e) Utilization of glucose

(f) Plasma glucagon

Figure 3.1: *Output of the three simulations. The first simulation shows the insulin injected before eating, after which the glucose appearance started. The second simulation is the situation, where the insulin is injected after eating the meal. The third simulation, the meal is delayed. The insulin is injected and the meal appears minutes later. As input signal the rate of appearance is given. The input is shown in the right upper plane.*

4 Parameter estimation

In Table 2.1, there are 35 parameters that need to be estimated. The other 28 are output values and are calculated by the model. This is a large number of parameters and can't be estimated at once all together. Estimation of the glucagon subsystem was approached first. The glucagon subsystem comprises of the subcutaneous administration of the glucagon, the glucagon kinetics in the plasma and the glucagon secretion by the α-cells. With the available clinical data provided by the study of Blauw et al. the glucagon secretion by the α-cells cannot be estimated [3]. The glucagon estimation is done for the subcutaneous administration and the plasma glucagon.

The clinical data considered 6 T1DM patients, who each visited a clinical research centre three times. Patients underwent a glucose clamp procedure to establish a certain blood glucose level during these visits. When the required blood glucose level was reached, a glucagon dose was administered. A blood sample was taken to analyze the glucagon pharmacokinetics every $10\ minutes$. 4 tests per visit were performed. The study schedule is shown in Table 4.1. For every subject there are 12 measurements.

9 data points were collected during each measurement. For one measurement the data points are depicted in red in Figure 4.1. The y-values are the glucagon concentration in the blood and were shifted, so that the y_0 starts at 0. This means $y_0 = 60.8$ is substracted from every y-value At $t = 0$ the glucagon was subcutaneously administered and data points were collected every $10\ minutes$.

Table 4.1: *The schedule for the glucagon data collection in the study [3].*

Visit	Blood glucose level $(mmol/L)$	Glucagon dose (mg)	Blood glucose level $(mmol/L)$	Glucagon dose (mg)	Blood glucose level $(mmol/L)$	Glucagon dose (mg)	Blood glucose level $(mmol/L)$	Glucagon dose (mg)
A	8	0.11	6	0.11	4	0.11	2.8	1.0
B	8	0.22	6	0.22	4	0.22	2.8	0.66
C	8	0.44	6	0.44	4	0.44	2.8	0.33

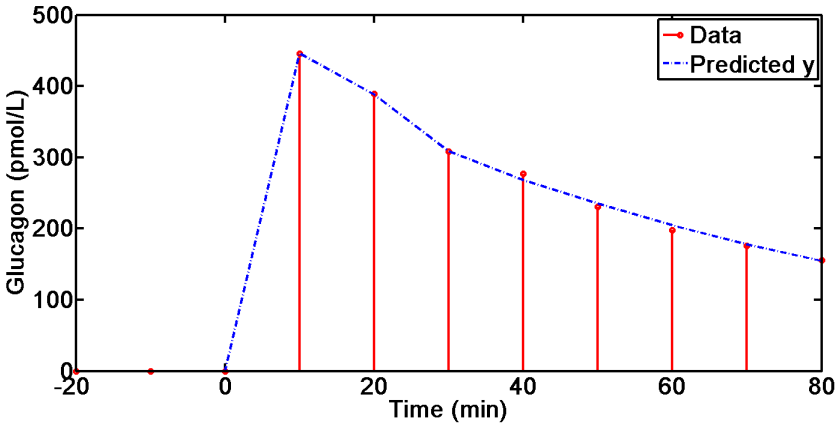

Figure 4.1: *The scaled glucagon data of one measurement and the new calculated y from the parameter estimation.*

These three differential equation were used for the parameter estimation:

$$\begin{cases} \dot{C}_{hp}(t) = -nC_{hp}(t) + S_h(t) + b_{p1}q_{Hsc1}(t) & \text{(4.1a)} \\ \dot{q}_{Hsc1}(t) = HIR(t) - b_{p1}q_{Hsc1}(t) - d_h q_{Hsc1}^{\frac{2}{3}}(t) & \text{(4.1b)} \\ \dot{q}_{Hsc2}(t) = d_h q_{Hsc1}^{\frac{2}{3}} - b_{p2}q_{Hsc2}. & \text{(4.1c)} \end{cases}$$

These are Eqs. (2.14a) and (2.14b) as mentioned in the section 2.3.2. The Eq. (2.14c) is substituted in to Eq. (2.12), which gives Eq. (4.1a).

Due to the power of $\frac{2}{3}$, the equations are non-linear. The equations were linearized by the Taylor polynomial method in the equilibrium point to estimate the parameters (b_{p1}, b_{p2}, d_h, n) in Eqs. (4.1a), (4.1b) and (4.1c). This equilibrium point is found by setting the input to 0, when there is no glucagon subcutaneously administered. The equilibrium point is represented in Eq. (4.2).

$$C_{hp,eq} = (\frac{d_h}{-b_{p1}})^3 \tag{4.2}$$

With the Eqs. (4.1a), (4.1b) and (4.1c) the following transfer function from the input HIR to the output C_{hp} was found:

$$H = \frac{2b_{p2}d_h^4}{b_{p1}^3(b_{p2}+s)(n+s)(b_{p1}+3s)}. \tag{4.3}$$

With this transfer function the parameters can be estimated using the ARX method in Matlab. This function uses the least squares method. The transfer function shows that the A-polynomial, the denominator in the fraction, is of the third order. The

B-polynomial, the numerator of the fraction, is a zero order polynomial. The ARX mathematical representation is:

$$y_k = \frac{B(z)}{A(z)}u_k + \frac{1}{A(z)}e_k. \tag{4.4}$$

Furthermore, there is a delay in the input-output relation. This can be seen in the data of Figure 4.1. The input starts at t_0 and the first output is seen at t_1. This accounts for a delay of one sample time and limits the possibilities of the estimation. As presented in Figure 4.1, 2 data points are added in the past. The estimation with ARX is an estimation in the z-transform. The ARX needs data points in the past, due to the order of the A-polynomial. These extra data points are assumed to be zero, because the system reacts after the given input. For the z-transform the following equations present the polynomial of the ARX in this case:

$$\begin{cases} A(z) = 1 + a_1 z^{-1} + a_2 z^{-2} + a_3 z^{-3} & \text{(4.5a)} \\ B(z) = b_0. & \text{(4.5b)} \end{cases}$$

The estimation is performed in Matlab and is presented in Figure 4.1. The blue dashed line is the new y-values for the estimated parameters and follows the data points. This is an example of one measurement in a single subject. There are 12 data sets for each patient where the conditions vary. As indicated in Table 4.1 the blood glucose levels and the glucagon dosages are different for every measurement. The estimation as described above were done for every data set. These different conditions need to indicate if the parameters are dependent on the blood glucose value or the glucagon dosages. The three A-polynomial parameter values (a_1, a_2, a_3) with their standard deviation are plotted in Figure 4.2. At this point the parameter of the B-polynomial is leaved out of consideration. There are 12 measurements shown in Figure 4.2 all from 1 subject. The parameters show a varied pattern. This indicates that the conditions of the measurements influence the model parameters. The ideal pattern is a horizontal line, this indicates than that the blood glucose and glucagon dosage does not influence the glucagon pharmacokinetics in 1 patient.

Looking at Figure 4.1 the estimation seems a good representation of the data. Only, the parameters values that are estimated to describe the results are complex numbers. This is inconsistent with the model equations. The expectation is that the human physiology is described by real numbers instead of complex numbers. The results with complex numbers are a structurally estimation error and appears in all measurements and in all subject.

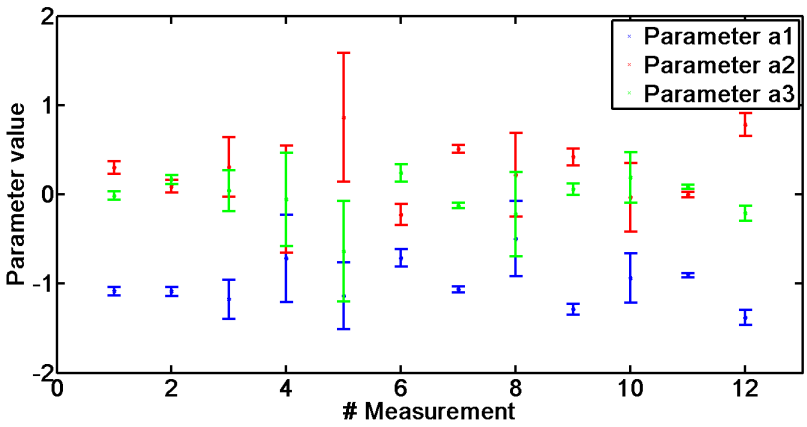

Figure 4.2: *Parameters of A-polynomial (a_1, a_2, a_3) with the standard deviation for 1 subject the 12 measurements are present.*

5 Discussion

This study provides insight in the human glucose regulation by designing a simulation model to test the algorithm of the AP of Inreda Diabetic BV. A simulation model was designed to test the algorithm of the AP of Inreda Diabetic BV. This model represents the glucose regulation system of T1DM patients. This representation is achieved by modeling three main physiological subsystems, the glucose, insulin and glucagon dynamics. For all the subsystems the physiological processes are explained. In addition, a major part of this study was obtaining the mathematical representation of the physiology. First simulation results proved that the model can simulate the glucose regulation, albeit with parameters from the literature.

5.1 Glucose

The glucose subsystem is described in several parts, namely the glucose regulation by the liver, the blood plasma glucose, the glucose utilization and absorption of glucose. The liver plays an important role in the glucose regulation and when diabetes progresses, the regulation by the liver changes [24]. This crucial role justifies to model the liver as a separate part. The EGP is influenced by glucose and two hormones, insulin and glucagon. The effects of the two hormones on the EGP are described by ODEs. Insulin's effect is described by two ODEs and the effect of glucagon is described by one ODE. In Figure 3.1c, the inhibition of EGP by glucose seems the strongest regulator. When the insulin is administered after the appearance of glucose, simulation 2, hardly any difference is seen in the decrease of EGP between simulation 1 and simulation 2. This is in contrast with the study of Dalla Man et al. [13]. Besides this, the stimulating effect of glucagon on EGP seems lower than the inhibiting effect of glucose and insulin together. The EGP is increased by glucagon, but this effect is not as strong as the decrease of EGP by glucose. This indicates that the implementation of EGP in the model might need adjustments to balance the influences on EGP of glucose and both hormones.

The glucose utilization is represented by the well-known Michaelis-Menten equation. This standard equation described the glucose transport into a cell by the GLUT-4 transporters. Figure 3.1e shows a good response to the insulin. It responses mainly to insulin and only slightly to glucose. The glucose utilization model could be expanded

by including physical activity. In section 2.1.2 the muscles and adipose tissues are assumed the same and the effect of physical activity was omitted. Nevertheless, physical activity has a major effect on the glucose utilization [5, 14, 30] and should be implemented in this model. The adipose tissue and muscles should be modeled separately. The GLUT-4 transporters in myocytes migrate under the influence of insulin and by contracting the muscles [29]. The response to this contraction depends on the intensity level of the physical activity. The GLUT-4 migration by the contracting muscles influences the Michaelis-Menten curve and should be implemented in the model. The process of gluconeogenesis in the liver is important during prolonged fasting and it becomes beneficial during physical activity. The glycogen source is rapidly exhausted by the energy demand of the muscles. If the physical activity is implemented in the model the contribution of gluconeogenesis has to be investigated.

The part that was not described in the chapter 2 is the GI tract. This must be modeled to simulate the glucose regulation in T1DM patient for different meals. Modeling of the GI tract can be done using compartments, i.e. considering the liquid and solid phase and the content of the meal. These influence the gastric emptying and therefore the glucose absorption in the blood plasma. This method is implemented in the study of Dalla Man et al. [13]. Another possible method is the simulation of glucose absorption from the food according to the glycemic index. The glycemic index ranks the carbohydrates in food by the extent to which they raise blood glucose levels after eating on a scale from 0 to 100 [18]. Food with a higher peak in postprandial blood glucose and a greater elevated blood glucose level, two hours after the intake, has a high glycemic index. These carbohydrates are rapidly digested and absorbed, hence result in fluctuating blood glucose levels. Food with a low glycemic index is slowly digested and absorbed, resulting in a lower peak and a steady rise of the blood plasma. An attempt was made to simulate the glucose absorption using the glycemic index. However, connecting the GI tract to the glucose subsystem proved to be difficult. The meal volume settings and the meal glycemic index seems to be inaccurate. The rate of glucose appearance in the blood plasma was mainly affected by the meal volume and less by the glycemic index of the meal. The expectation is that the glycemic index mainly determines the glucose appearance in the blood plasma. Therefore, changing the parameter settings could be a solution. Otherwise the mathematical submodel of the GI tract should be reconsidered.

5.2 Insulin

At this moment, the AP is designed for and tested with T1DM patients, however the AP might also treat type 2 diabetes mellitus (T2DM) patients in the future. At this point the model does not contain β-cells, because the pancreatic insulin secretion

is assumed to be zero for T1DM patients. Ideally, the AP will be tested with the simulation model, before the clinical trials with T2DM. β-cell must be modeled to perform this simulation. It is important to consider the two phasic secretion of insulin by β-cells [4, 36]. The first phase is a fast insulin release and the second phase a slower insulin release. Although the secretion phases are impaired in T2DM patients [26], both phases still need to be modeled. The plasma insulin in T2DM patients still shows the two phased secretion. The liver also contributes to the insulin regulation [6, 35]. The anatomical location of the liver and the pancreas results in the insulin extraction by the liver. Not all the secreted insulin will reach the rest of the body. This regulation by the liver is already implemented in the model, which makes the extension of β-cell a small step.

The subcutaneous route of insulin is implemented with a spherical release of the administered insulin. The study of Lv et al. concludes that the subcutaneous administration route shows a delayed clearance of insulin and a biphasic appearance in the blood plasma [25]. The delayed clearance is partly met by the spherical release in the model, due to the slower absorption. Simulation with a spherical release shows that the administered insulin is longer present in the blood plasma. The biphasic appearance is not simulated and can be implemented by a fourth order polynomial. This makes the model more complex and affects the parameter estimation for this part of the model. The data has to be sufficiently rich, e.g. contain the biphasic appearance to estimate the unknown parameters. The available clinical data cannot describe the unknown parameters [7]. The spherical release is the best solution to this point.

Figure 3.1d shows the rise in the plasma insulin and a return back to zero after $1.5\ hours$. This is a quickly return compared to other studies [12, 25] and seems unrealistic. Insulin used in the AP has a duration of effectiveness between 2 and 5 $hours$. The simulated insulin in the plasma is cleared in 2 $hours$ and is faster than expected. Next, the simulation used 100 $units$ of administered insulin. This is an unlikely amount of insulin. The parameters values found in the literature can cause this effect. Using other parameter settings might slow the insulin clearance.

5.3 Glucagon

As mentioned in chapter 1, the glucagon kinetics and dynamics are important to simulate in the model. The review of Wilinska et al. and the review of Colmegna et al. indicate that there was no existing model that simulates the glucagon subsystem [11, 38]. After the published reviews, the UVA/Padova model is expanded by including the glucagon kinetics and dynamics. Since the extension of this model is based on

non-published assumptions, there is uncertainty about its accuracy. In this study the designed model for testing the AP also considers the glucagon part for the simulation. Compared to the UVA/Padova model the subcutaneous administration for glucagon is added in the same way as the subcutaneous administration for insulin in this study. In addition, the glucagon secretion by the α-cells are differently modeled. This is a second difference to the UVA/Padova model. The results show the glucagon secretion, which consists of the static and dynamic secretion as explained in section 2.3.1. The static part reacts on the plasma glucose concentration and the dynamic part to the change of plasma glucose concentration. This is in consistence with the insulin secretion modeled in other studies [4, 13, 26, 36] and the base for the α-cell secretion. Figure 3.1f indicates that the glucagon secretion is primarily regulated by the dynamic part. This is shown in the last part of the curve after $4\ hours$ where the secretion increases. This increase is the result of the secretion stimulated by the dynamic part of the glucagon secretion. The dynamic part reacts on the change of the glucose level. This indicates that the dynamic part of the secretion reacts on the fluctuations in the blood glucose, even if there is hyperglycaemia. The glucagon secretion in this model should be reconsidered. Furthermore, the insulin level inhibits the glucagon secretion. This negative feedback is not covered by mathematical representation.

The effect of glucagon on EGP is shown in Figure 3.1c in the third simulation. It shows an increase in EGP as reaction to the increased glucagon secretion. Only, the result of the increased EGP on the blood plasma glucose is not clearly seen in Figure 3.1a. The increase of the glucose concentration in the blood plasma seems to be a result of the glucose appearance after the intake of carbohydrates instead of an increase of EGP. The expectation was that the EGP is able to drive the glucose level back to the steady state. A possible explanation for the weak reaction is the use of the parameters values for this simulation. The parameters are based on the literature. The parameters for the glucagon part are provided by another study than the parameters of the other model parts. This can explain the weak reaction to the glucagon concentration, because the parameters are not estimated based on the same clinical data.

5.4 Parameters

At this moment the model consists of 35 parameters, which may increase as the model changes. Ideally these parameters all need to be estimated. However, this is difficult due to the poorly available clinical data. Therefore, some parameters are searched for in the available literature. Notice that these are mostly the mean values for a parameter. To provide the inter and the possible intra patient differences,

using the mean values for the parameters is unreliable. A first step was made to estimate the parameters of the model. The estimation started with the glucagon part. This choice was made due to the available clinical data. This study used the ARX method to estimate the parameters, which uses the linear least square method. Surprisingly, this method provides complex numbers, which was not to be expected. Physiologically, the parameter values are real numbers. According to the fit, represented in Figure 4.2, it seemed a good method. The first attempt indicates that the parameter estimations are not straightforward and that further work should focus on the estimation of the parameters.

A possibility can be to force the ARX method to return real values. Another possibility is reconsidering the method to estimate the parameters. Alternatively, the Output-Error method was tried, this is another method to estimate the parameters. This method does not consider the disturbance to the system. It assumes that the disturbance is a white noise signal. The Output-Error method gave similar values for the estimated parameters as the ARX model gave. And the fit does not show a great difference to the ARX fit. The ARX method was chosen, because it considered the disturbance term $\frac{1}{A(z)}e_k$. The disturbance is important to account for, because because in the model, different assumptions were made and the collection of the data is expected to cause disturbance in the model. This disturbance is also part of the estimation.

It is a challenge to acquire the necessary clinical data. In general, the data has to be rich enough to contain the unknown parameters for the estimation. The data need to be sufficiently rich for the model considered. The clinical data might be enriched by measuring additional variables. Finding clinical data for the submodels as the liver and utilization and the secretion of both hormones will be difficult. For example, to estimate the EGP parameters it is ideally required to known the plasma glucose in the portal vein and the plasma glucose in the hepatic vein. In this way the effect of the EGP can be estimated by the change of the glucose level.

6 Conclusion

This study provides a substantial basis for the in silico testing of the AP developed by Inreda Diabetic BV. The model provides more insight in the human glucose regulation and can be helpful in the development and testing processes for the AP. The model represents the glucose regulation system in T1DM patients. The model consist of 10 submodels, that describe the three main physiological subsystems, the glucose, insulin and glucagon processes. These processes are described by fifteen differential equations and the seven mathematical equations. In total there are 35 parameters and 28 outputs. First simulation results proved that the model can simulate the glucose regulation. Therefore, this model is a valuable tool for preclinical testing of the AP.

Bibliography

[1]B. W. Bequette. “A critical assessment of algorithms and challenges in the development of a closed-loop artificial pancreas”. In: *Diabetes technology & therapeutics* 7.1 (2005), pp. 28–47 (cit. on p. 5).

[2]H. Blauw, A.C. van Bon, R Koops, and J.H. DeVries. “Performance and sagety of an integrated bihormonal artificial pancreas for fully automated glucose control at home”. In: *Diabetes, Obesity and Metabolism* 18.March (2012), pp. 671–677 (cit. on p. 3).

[3]H. Blauw, I. Wendl, J. H. Devries, T. Heise, and T. Jax. “Pharmacokinetics and pharmacodynamics of various glucagon dosages at different blood glucose levels”. In: *Diabetes, Obesity and Metabolism* 18.1 (2016), pp. 34–39 (cit. on pp. 6, 33).

[4]E. Breda, M. K. Cavaghan, G. Toffolo, K. S. Polonsky, and C. Cobelli. “Oral glucose tolerence test minimal model indexes of beta-cell function and insulin sensitivity”. In: *Diabetes* 50.1 (2001), pp. 150–158 (cit. on pp. 39, 40).

[5]M. D. Breton. “Physical Activity: the major unaccounted impediment to closed loop control”. In: *Journal of Diabetes Science and Technology* 2.1 (2008), pp. 169–174 (cit. on p. 38).

[6]M. Campioni, G. Toffolo, R. Basu, R. A. Rizza, and C. Cobelli. “Minimal model assessment of hepatic insulin extraction during an oral test from standard insulin kinetic parameters.” In: *American Journal of Physiology Endocrinology and Metabolism* 297 (2009), E941–E948 (cit. on p. 39).

[7]E. Carson and C. Cobelli. *Modelling methodology for physiology and medicine*. 2001. arXiv: `arXiv:1011.1669v3` (cit. on pp. 3, 39).

[8]L. J. Chassin, M. E. Wilinska, and R. Hovorka. “Evaluation of glucose controllers in virtual environment: methodology and sample application.” In: *Artificial intelligence in medicine* 32.3 (2004), pp. 171–81 (cit. on p. 4).

[9]M. Cnop, N. Welsh, J. Jonas, A. Jo, and S. Lenzen. “Mechanisms of pancreatic beta-cell death in Type 1 and Type 2 diabetes”. In: *Diabetes* 54.2 (2005), pp. 97–107 (cit. on p. 1).

[10]Cl. Cobelli and E. Carson. “Chapter 1 Introduction”. In: *Introduction to modeling in Physiology and Medicine*. 2008, pp. 1–2 (cit. on p. 3).

[11]P. Colmegna and R. S. Sánchez Peña. “Analysis of three T1DM simulation models for evaluating robust closed-loop controllers”. In: *Computer Methods and Programs in Biomedicine* 113.1 (2014), pp. 371–382 (cit. on pp. 4, 39).

[12]C. Dalla Man, D. M. Raimondo, R. A. Rizza, and C. Cobelli. “GIM , Simulation software of meal glucose-insulin Model”. In: *Journal of Diabetes Science and Technology* 1.3 (2007), pp. 1–8 (cit. on p. 39).

[13]C. Dalla Man, R. A. Rizza, and C. Cobelli. “Meal simulation model of the glucose-insulin system”. In: *IEEE transactions on bio-medical engineering* 54.10 (2007), pp. 1740–1749 (cit. on pp. 12, 29, 37, 38, 40).

[14]C. Dalla Man, M. D. Breton, and C. Cobelli. “Physical activity into the meal glucose–insulin model of type 1 diabetes: in silico studies”. In: *Journal of Diabetes Science and Technology* 3.1 (2009), pp. 56–67 (cit. on p. 38).

[15]C. Dalla Man, F. Micheletto, D. Lv, et al. “The UVA/PADOVA type 1 diabetes simulator: new features.” In: *Journal of Diabetes Science and Technology* 8.1 (2014), pp. 26–34 (cit. on p. 6).

[16]R. L. Dobbins, S. N. Davis, D. W. Neal, et al. “Compartmental modeling of glucagon kinetics in the conscious dog”. In: *Metabolism* 44.4 (1995), pp. 452–459 (cit. on p. 21).

[17]F. H. El-Khatib, S. J. Russell, D. M. Nathan, R. G. Sutherlin, and E. R. Damiano. “Bihormonal closed-loop glucose control for type 1 diabetes”. In: *Science Translational Medicine* 2.27 (2010), pp. 1–17 (cit. on p. 3).

[18]K. Foster-Powell, S. H. A. Holt, and J. C. Brand-Miller. “International table of glycemic index and glycemic load values”. In: *The American Journal of Clinical Nutrition* 76.2 (2002), pp. 5–56 (cit. on p. 38).

[19]E. I. Georga, V. C. Protopappas, C. V. Bellos, and D. I. Fotiadis. “Wearable systems and mobile applications for diabetes disease management”. In: *Health and Technology* 4.2 (2014), pp. 101–112 (cit. on pp. 1–3).

[20]E. Gylfe and P. Gilon. “Glucose regulation of glucagon secretion”. In: *Diabetes Research and Clinical Practice* 103.1 (2014), pp. 1–10 (cit. on p. 3).

[21]V. Hagger, C. Hendrieckx, J. Sturt, T. C. Skinner, and J. Speight. “Diabetes distress among adolescents with type 1 diabetes: a systematic review”. In: *Current Diabetes Reports* 16.1 (2016), pp. 1–14 (cit. on p. 1).

[22]L. Heinemann, L. Hirsch, and R. Hovorka. “Lipohypertrophy and the artificial pancreas: is this an issue?” In: *Journal of diabetes science and technology* 8.5 (2014), pp. 915–7 (cit. on p. 2).

[23]E. J. Henriksen. “Exercise effects of muscle insulin signaling and action. Invited Review: Effects of acture exercise and exercise training on insulin resistance”. In: *Journal of Applied Physiology* 93 (2002), pp. 788–796 (cit. on p. 17).

[24]K. M Krudys, M. G. Dodds, S. M. Nissen, and P. Vicini. “Integrated model of hepatic and peripheral glucose regulation for estimation of endogenous glucose production during the hot IVGTT”. In: *American Journal of Physiology Endocrinology and Metabolism* 288 (2005), pp. 1038–1046 (cit. on pp. 13, 37).

[25]D. Lv, S. D. Kulkarni, A. Chan, et al. “Pharmacokinetic Model of the Transport of Fast-Acting Insulin From the Subcutaneous and Intradermal Spaces to Blood”. In: *Journal of Diabetes Science and Technology* 9.4 (2015), pp. 831–840 (cit. on p. 39).

[26]J. J. Meier, J. D. Veldhuis, and P. C. Butler. “Pulsatile insulin secretion dictates systemic insulin delivery by regulating hepatic insulin extraction in humans”. In: *Diabetes* 54 (2005), pp. 1649–1656 (cit. on pp. 19, 39, 40).

[27]M. C. Moore, C. C. Connolly, and A. D. Cherrington. “Autoregulation of hepatic glucose production”. In: *European Journal of Endocrinology* 138.3 (1998), pp. 240–248 (cit. on p. 13).

[28]S. Pellegrini, E. Cantarelli, V. Sordi, R. Nano, and L. Piemonti. “The state of the art of islet transplantation and cell therapy in type 1 diabetes”. In: *Acta Diabetologica* (2016) (cit. on p. 1).

[29]Erik A Richter and Mark Hargreaves. “Exercise, GLUT4, and skeletal muscle glucose uptake”. In: *Physiological Reviews* 93.3 (2013), pp. 993–1017 (cit. on pp. 17, 38).

[30]A. Roy and R. S. Parker. “Dynamic modeling of exercise effects on plasma glucose and insulin levels”. In: *Journal of Diabetes Science and Technology* 1.3 (2007), pp. 338–347 (cit. on p. 38).

[31]P. R. Shepherd and B. B. Kahn. “Glucose transporters and insulin action. Implications for insulin resistance and diabetes mellitus”. In: *The New England Journal of Medicine* 341.4 (1999), pp. 248–257 (cit. on p. 16).

[32]J. S. Skyler. “T1DM in 2014: Progress towards a bionic pancreas.” In: *Nature reviews. Endocrinology* 11.2 (2015), pp. 75–6 (cit. on p. 3).

[33]G.M. Steil, B. Clark, S. Kanderian, and K. Rebrin. “Modeling insulin action for development of a closed-loop artificial pancreas”. In: *Diabetes technology & therapeutics* 7.1 (2005), pp. 94–108 (cit. on p. 5).

[34]H. L. Stuckey, C. Mullan-Jensen, S. Kalra, et al. “Living with an adult who has diabetes: qualitative insights from the second diabetes attitudes, wishes and needs (DAWN2) study”. In: *Diabetes Research and Clinical Practice* 116 (2016), pp. 270–278 (cit. on p. 1).

[35]G. Toffolo, M. Campioni, R. Basu, R. A. Rizza, and C. Cobelli. “A minimal model of insulin secretion and kinetics to assess hepatic insulin extraction”. In: *American Journal of Physiology Endocrinology and Metabolism* 290.1 (2006), pp. 169–176 (cit. on p. 39).

[36]G. Toffolo, E. Breda, M. K. Cavaghan, et al. “Quantitative indexes of beta-cell function during graded up & down glucose infusion from C-peptide minimal models”. In: *American Journal of Physiology Endocrinology and Metabolism* 280.43-1 (2001), pp. 2–10 (cit. on pp. 39, 40).

[37]T. Van Belle, K. Coppieters, and M. Von Herrath. “Type 1 diabetes: etiology, immunology, and therapeutic strategies”. In: *Physiological Reviews* 91 (2011), pp. 79–118 (cit. on p. 1).

[38]M. E. Wilinska and R. Hovorka. “Simulation models for in silico testing of closed-loop glucose controllers in type 1 diabetes”. In: *Drug Discovery Today: Disease Models* 5.4 (2008), pp. 289–298 (cit. on pp. 4, 39).

[39]Z. Wu, C. K. Chui, G. S. Hong, E. Khoo, and S. Chang. “Glucose-insulin regulation model with subcutaneous insulin injection and evaluation using diabetic inpatients data”. In: *Computer Methods and Programs in Biomedicine* 111.2 (2013), pp. 347–56 (cit. on p. 12).

Acknowledgements

You are reading the result of one year of hard work. I could not reach this achievement without the support of my supervisors. I would like to thank Hans Zwart for our many conversations and his patience trying to educate me in the area of mathematics. Arianne van Bon, thank you for your guidance and medical knowledge. During setbacks I could always count on Marleen Groenier. And of course Helga Blauw with whom I cooperated last year, resulting in fruitful discussions and many new insights.

Needing the occasional relaxation, I could always count on my good friends Marije Kamphuis and Xenia Hoppenbrouwer. Thank you for letting me get off some steam and thank you for your valuable feedback.

I want to thank mom and dad for supporting me during my life as a student. I always had a place to go to. And finally Daan Visscher, who keeps getting to put up with me. Thanks for your love and supports.

Appendix A

Table 6.1: *The parameters values used for the simulations.*

Abbreviation	Value	Unity
a_{p1}	0.5	min^{-1}
a_{p2}	0.13	min^{-1}
b_{p1}	0.03	min^{-1}
b_{p2}	0.09	min^{-1}
$C_{hp,b}$	50	ng/L
$C_{ip,b}$	2.48	$pmol/L$
d_h	2.05	min^{-1}
d_i	0.081	min^{-1}
E	0	$mg/kg/min$
EGP_0	2.5	$mg/kg/min$
F	1.1	$mg/kg/min$
h	98.94	mg/dL
k_1	0.065	min^{-1}
k_2	0.079	min^{-1}
k_{ge}	0.0021	min^{-1}
k_{hd}	0.093	min^{-1}
k_{hl}	0.05	$mg/kg/min\ per\ ng/L$
k_{id}	0.0079	min^{-1}
k_{il}	0.009	$mg/kg/min\ per\ pmol/L$
K_{m0}	225.59	mg/kg
m_1	0.190	min^{-1}
m_2	0.484	min^{-1}
m_4	0.194	min^{-1}
m_5	0.0304	min^{-1}
m_6	0.6471	min^{-1}
n	0.22	min^{-1}
p	0.0331	min^{-1}
$S_{h,b}$	5	$ng/kg/min$
V_{m0}	2.50	$mg/kg/min$

Table6.1 – continued from previous page

Abbreviation	Value	Unity
V_{mcii}	0.047	$mg/kg/min\,per\,pmol/L$
δ	3.01	$ng/L\ per\ mg/dL$
ρ	0.86	min^{-1}
σ	0.41	$ng/L/min$